AUTHOR QUERY FORM

ELSEVIER	**Journal: YJMCC** **Article Number: 7338**	**Please e-mail or fax your responses and any corrections to:** **E-mail: corrections.essd@elsevier.spitech.com** **Fax: +1 619 699 6721**

Dear Author,

Please check your proof carefully and mark all corrections at the appropriate place in the proof (e.g., by using on-screen annotation in the PDF file) or compile them in a separate list. Note: if you opt to annotate the file with software other than Adobe Reader then please also highlight the appropriate place in the PDF file. To ensure fast publication of your paper please return your corrections within 48 hours.

For correction or revision of any artwork, please consult http://www.elsevier.com/artworkinstructions.

Any queries or remarks that have arisen during the processing of your manuscript are listed below and highlighted by flags in the proof. Click on the 'Q' link to go to the location in the proof.

Location in article	**Query / Remark: click on the Q link to go** **Please insert your reply or correction at the corresponding line in the proof**
Q1	Please confirm that given names and surnames have been identified correctly.
Q2	The country name "Italy" has been inserted for the second affiliation. Please check, and correct if necessary.
Q3	Funding was modified to Acknowledgments. Please check if appropriate.
Q4	Please provide a caption.
Q5	Uncited reference: This section comprises references that occur in the reference list but not in the body of the text. Please position each reference in the text or, alternatively, delete it. Thank you. Please check this box if you have no corrections to make to the PDF file. ☐

Thank you for your assistance.

YJMCC-07338; No. of pages: 1; 4C:

Journal of Molecular and Cellular Cardiology xxx (2012) xxx

Contents lists available at SciVerse ScienceDirect

Journal of Molecular and Cellular Cardiology

journal homepage: www.elsevier.com/locate/yjmcc

Highlights

Journal of Molecular and Cellular Cardiology xxx (2012) xxx–xxx

A caveolin-binding domain in the HCN4 channels mediates functional interaction with caveolin proteins

Andrea Barbuti [a,b,*], Angela Scavone [a], Nausicaa Mazzocchi [a], Benedetta Terragni [a], Mirko Baruscotti [a,b], Dario DiFrancesco [a,b]

[a] *Department of Biomolecular Sciences and Biotechnology, The PaceLab, Università degli Studi di Milano, via Celoria 26, 20133 Milano, Italy*
[b] *Centro Interuniversitario di Medicina Molecolare e Biofisica Applicata (CIMMBA), University of Milano, Italy*

► Mutations in the HCN4 caveolin-binding domain (CBD) affect channel kinetics. ► Mutated channels are insensitive to caveolar disorganization. ► Trafficking of mutated channels to the plasma membrane is impaired. ► Mutated channels show a weaker interaction with caveolin-1. ► Reconstitution of the CBD makes the channels similar to the wild type.

0022-2828/$ – see front matter © 2012 Published by Elsevier Ltd.
doi:10.1016/j.yjmcc.2012.05.013

Q4 Supplementary Fig. 1 HCN4 channels have a conserved CBD. schematic representation of one HCN4 subunit formed by six transmembrane domains (S1-6), intracellular N- and C-termini and a cAMP binding domain (CNBD). The inset shows the position of the CBD (white letters), in the amino acid sequence (top). Bottom, the CBD sequence (grey background) is fully conserved in urochordates and vertebrates but is lost in invertebrates.

Supplementary Fig. 2 Expression of caveolin proteins in CHO and caveolin-free mef cells. Single confocal images showing the expression of endogenous cav-1 (red) in CHO cells (top) and the lack of any detectable cav-1 signal in caveolin-free mef (bottom). Nuclei stained by DAPI; calibration bars 20 μm. The western blot shown in the lower panel confirms the lack of any signal for both cav-1 and cav-3 in caveolin-free mef and the expression of cav-1 by CHO cells; a protein lysate from mouse ventricle was used as positive control.

Supplementary Fig. 3 Effect of MβCD treatment on WT-HCN4 channel trafficking. Confocal images of untreated and MβCD-treated CHO cells transfected with WT HCN4 construct (green). Nuclei stained by DAPI; calibration bars 10 μm.

Supplementary Fig. 4 Caveolin-scaffolding domain is highly conserved. Comparison of sequences of the caveolin-scaffolding domain of cav-1, -3 and of caveolin-related proteins of vertebrates, urochordates and invertebrates.

Supplementary Table 1 Mean values of half activation voltages ($V_{1/2}$), inverse slope factors (s), activation (-85 mV) and deactivation (-45 mV) τ of WT and mutant HCN4 currents. Number of cells for each group is indicated in parentheses. Asterisks denote statistically significant differences ($p<0.05$).

Supplementary Table 3 cAMP sensitivity of WT and mutated HCN4 channels. Mean half activation voltage ($V_{1/2}$) and inverse slope factor (s) values in the presence of 10 μM cAMP in the pipette solution and in day-matched controls. Number of cells for each group is indicated in parentheses.

Supplementary Table 2 Mean values of $V_{1/2}$, s and deactivation τ of MβCD-treated and day-matched untreated HCN4 and HCN1 currents. Number of cells for each group is indicated in parentheses. Asterisks denotes $p<0.05$.

Supplementary Table 4 Primers used to generate mutant HCN4 channels

Journal of Molecular and Cellular Cardiology xxx (2012) xxx–xxx

Contents lists available at SciVerse ScienceDirect

Journal of Molecular and Cellular Cardiology

journal homepage: www.elsevier.com/locate/yjmcc

Original article

A caveolin-binding domain in the HCN4 channels mediates functional interaction with caveolin proteins

Andrea Barbuti [a,b,*,1], Angela Scavone [a,1], Nausicaa Mazzocchi [a,2], Benedetta Terragni [a,3], Mirko Baruscotti [a,b], Dario DiFrancesco [a,b]

[a] Department of Biomolecular Sciences and Biotechnology, The PaceLab, Università degli Studi di Milano, via Celoria 26, 20133 Milano, Italy
[b] Centro Interuniversitario di Medicina Molecolare e Biofisica Applicata (CIMMBA), University of Milano, Italy

ARTICLE INFO

Article history:
Received 13 January 2012
Received in revised form 18 April 2012
Accepted 10 May 2012
Available online xxxx

Keywords:
HCN
Pacemaker channels
Caveolae
Caveolin binding domain
Trafficking
Subcellular localization

ABSTRACT

Pacemaker (HCN) channels have a key role in the generation and modulation of spontaneous activity of sinoatrial node myocytes. Previous work has shown that compartmentation of HCN4 pacemaker channels within caveolae regulates important functions, but the molecular mechanism responsible is still unknown. HCN channels have a conserved caveolin-binding domain (CBD) composed of three aromatic amino acids at the N-terminus; we sought to evaluate the role of this CBD in channel–protein interaction by mutational analysis. We generated two HCN4 mutants with a disrupted CBD (Y259S, F262V) and two with conservative mutations (Y259F, F262Y). In CHO cells expressing endogenous caveolin-1 (cav-1), alteration of the CBD shifted channels activation to more positive potentials, slowed deactivation and made Y259S and F262V mutants insensitive to cholesterol depletion-induced caveolar disorganization. CBD alteration also caused a significant decrease of current density, due to a weaker HCN4–cav-1 interaction and accumulation of cytoplasmic channels. These effects were absent in mutants with a preserved CBD.In caveolin-1-free fibroblasts, HCN4 trafficking was impaired and current density reduced with all constructs; the activation curve of F262V was not altered relative to wt, and that of Y259S displayed only half the shift than in CHO cells.The conserved CBD present in all HCN isoforms mediates their functional interaction with caveolins. The elucidation of the molecular details of HCN4–cav-1 interaction can provide novel information to understand the basis of cardiac phenotypes associated with some forms of caveolinopathies.

1. Introduction

The intrinsic spontaneous activity of sinoatrial node (SAN) makes this region the natural pacemaker of the heart. SAN action potentials are characterized by a slow diastolic depolarization which drives the membrane voltage toward the threshold for the firing of the subsequent action potential. The autonomic nervous system can induce acceleration or slowing of cardiac rhythm by increasing or decreasing, respectively, the steepness of diastolic depolarization [1,2]. A critical role in this phase is played by the pacemaker I_f current [3]; I_f flows through hyperpolarization-activated cyclic nucleotide-gated channels (HCN), of which four isoforms (HCN1-4) have been described [4]. Of the four isoforms, HCN4 is the most abundantly expressed in the SAN of different species including humans [5–8]. Combinatory expression of various HCN subunits can explain some but not all of the properties of the native I_f current [9], and it is now clear that much of the kinetic variability of the I_f current is due to the interaction of HCN channels with auxiliary subunits. In the heart, for example, HCN channel properties have been shown to be altered by interaction with caveolin-3 (cav-3), MiRP1, KCR1 and SAP97 proteins [10–15].

We and others [12,13] have shown that HCN4 co-localizes and interacts with cav-3 both in the rabbit SAN and in heterologous expression systems. Disruption of this interaction has a significant influence on spontaneous rate of SAN myocytes because it shifts the activation curve to more depolarized potentials and slows deactivation kinetics. In addition, caveolae disorganization affects the f-channel sensitivity to β-adrenergic stimulation, thus altering the physiological modulatory pathways of heart rhythm [12,16].

Caveolins are structural proteins of caveolae, membrane microdomains whose function is, among others, to co-localize within

Abbreviation: SAN, Sinoatrial node; HCN, hyperpolarization-activated cyclic nucleotide-gated; cav-1, caveolin-1; cav-3, caveolin-3; CBD, caveolin binding domain; MβCD, Methyl-β-cyclodextrin; V_{half}, half activation voltage; s, inverse-slope factors; τ, time constant; mef, mouse embryonic fibroblasts.

* Corresponding author at: Department of Biomolecular Sciences and Biotechnology, The PaceLab, Università degli Studi di Milano, via Celoria 26, 20133 Milano, Italy. Tel.: +39 02 50314941; fax: +39 02 50314932.
E-mail address: andrea.barbuti@unimi.it (A. Barbuti).
[1] These authors equally contributed to the work.
[2] Current address: Divisione di Scienze Metaboliche e Cardiovascolari, Istituto Scientifico San Raffaele, Via Olgettina 60, 20132 Milano, Italy.
[3] Current address: Istituto Neurologico C. Besta, Centro Epilessia, via Celoria 11, 20133 Milano, Italy.

0022-2828/$ – see front matter © 2012 Published by Elsevier Ltd.
doi:10.1016/j.yjmcc.2012.05.013

restricted spaces proteins involved in the same signaling pathway in order to facilitate their functional interactions [17]. Three caveolin isoforms are found in mammalian cells: while caveolin-1 (cav-1) is ubiquitously expressed and caveolin-3 (cav-3) is expressed mainly in smooth and striated muscles these two isoforms are highly conserved and functionally homologous [18,19]; caveolin-2 instead is usually co-expressed with cav-1 and in addition of being less conserved cannot form caveolae by itself. Several caveolar proteins directly interact with the conserved scaffolding domain of either cav-1 or cav-3 through a caveolin binding domain (CBD) composed of a series of correctly spaced aromatic residues (ΦXΦXXXXΦ, ΦXXXXΦXXΦ or ΦXΦXXXXΦXX, where Φ is Tyrosine (Y), Phenylalanine (F) or Tryptophan (W) and X any other amino acid [18]), which is found in all HCN channels.

Although native SAN myocytes express cav-3, we decided to investigate the molecular basis of the association between heterologously-expressed HCN4 channels and caveolin proteins in CHO cells which express cav-1. Mutations disrupting the CBD of the rabbit (rb)HCN4 isoform caused alterations in channel kinetics similar to those generated by chemically-induced caveolar disorganization, and strongly decreased channel expression at the plasma membrane.

2. Materials and methods

See SI Materials and methods for details.

2.1. HCN4 constructs

The rbHCN4 isoform in pCI (Promega) was used as template to generate mutated channels with the CBD either disrupted (Y259S, F262V) or maintained (Y259F, F262Y). All mutants were confirmed by direct sequencing.

2.2. Cell culture and transfection

CHO and Cav-1-free mouse embryonic fibroblasts (3T3 mef KO, ATCC) were transfected by Lipofectamine™ and Plus Reagent (Invitrogen) or with Fugene® (Promega), following manufacturer instructions.

2.3. Cholesterol depletion

Membrane cholesterol depletion was achieved by 1% methyl-β-cyclodextrin (MβCD, Sigma) treatment as previously described [16]. CHO cells were incubated for 2 h at room temperature in the MβCD-containing medium before electrophysiological or immunofluorescence analysis.

2.4. HCN4 distribution analysis

Transfected cells were fixed and stained with an anti-HCN4 antibody and channel distribution analyzed with a confocal microscope. Cellular distribution of WT and mutated HCN4 channels was compared by analyzing the membrane-to-cytosol fluorescence intensity ratio obtained as follows: 1) "mean brightness" (arbitrary unit of measurement) of HCN4 signal and the corresponding area (μm^2) for both the cytosolic and membrane compartments were measured using the NIS-Elements Basic Research 2.30 software (Nikon); 2) signal density was calculated as the ratio between brightness and area; 3) the density ratio was then calculated as the ratio between the corresponding cytosolic and membrane densities for each cell, and density ratio values were averaged and plotted (see Figs. 4C and D).

2.5. Co-immunoprecipitation and WB quantification

For co-immunoprecipitation, 0.5 mg (1 mg/ml) of proteins was used for each sample. The quantification of western blot signals was carried out using Image J (U. S. National Institutes of Health, Bethesda, Maryland, USA). We quantified the HCN4 signals derived from the immunoprecipitated blot with the anti-cav-1 antibody. Since the amount of HCN4 protein that can be precipitated depends on transfection efficiency, each HCN4 signal was normalized to the HCN4 signal in the corresponding lysate.

2.6. Electrophysiology and data analysis

I_{HCN4} and I_{HCN1} were activated by hyperpolarizing test steps to the range of −35/−135 mV for WT HCN4, Y259F and F262Y channels or to the range of −25/−125 mV for HCN4-Y259S, F262V and WT mHCN1 channels, followed by a fully activating step at −135 mV or −125 mV, respectively, from a holding potential of −20 mV. Each step was long enough to reach steady-state current activation.

2.7. Statistics

Statistical analysis was performed by Student's *t*-test for independent populations. Results were expressed as mean ± SEM Significance level was set to $p = 0.05$.

3. Results

3.1. HCN4 interacts with caveolins in both in SAN myocytes and in CHO cells

A putative CBD [18] composed of three aromatic residues is found at the N-terminus of all HCN isoforms and is conserved throughout the animal kingdom from urochordates to vertebrates (Supplementary Fig. 1). We thus hypothesized that interaction with caveolin is an essential feature of HCN function.

We have previously shown that HCN4 channels interact with cav-3 in native rabbit SAN myocytes [12]. We have also evaluated here the expression of cav-1 in mouse SAN myocytes. Immunofluorescence analysis of isolated SAN cells, stained with an anti-cav-3 and anti-cav-1 antibodies, showed clearly that this cell type express both isoforms of caveolin (Fig. 1A). Western blot analysis of SAN tissues (Fig. 1B, left) confirmed the expression of both cav-3 and cav-1, and co-immunoprecipitation experiments revealed that HCN4 interacts with both isoforms (Fig. 1B right).

To better investigate this interaction, we transfected the WT rbHCN4 channels into CHO cells, which express endogenous cav-1 (Supplementary Fig. 2). Cells lysates obtained from either non-transfected (nt) or HCN4-transfected (WT) cells were immunoprecipitated using anti-cav-1 (IP-cav-1) or anti-HCN4 (IP-HCN4) primary antibodies and checked for the presence of HCN4 or cav-1, respectively. In the western blot analysis of Fig. 2A, specific signals for HCN4 (160 kDa) and cav-1 (22 kDa) proteins were detected in all lanes corresponding to transfected cells. As expected, no HCN4 signal was detected in the IP-cav-1 from non-transfected cells, and neither HCN4 nor cav-1 signals were detected in the IP-HCN4 from non-transfected cells.

3.2. Mutation of the caveolin-binding domain of HCN4 alters channel kinetics

In order to evaluate the importance of the CBD in the HCN4–cav-1 interaction, we generated four mutated HCN4 constructs: in two of them the CBD was disrupted by substituting either the aromatic residues tyrosine 259 or phenylalanine 262 with a serine and a valine respectively (Y259S and F262V); in the other two mutants the CBD motif was maintained by introducing in the sequence an aromatic residue different from the original one (Y259F and F262Y).

Please cite this article as: Barbuti A, et al, Original articleA caveolin-binding domain in the HCN4 channels mediates functional interaction with caveolin proteins, J Mol Cell Cardiol (2012), doi:10.1016/j.yjmcc.2012.05.013

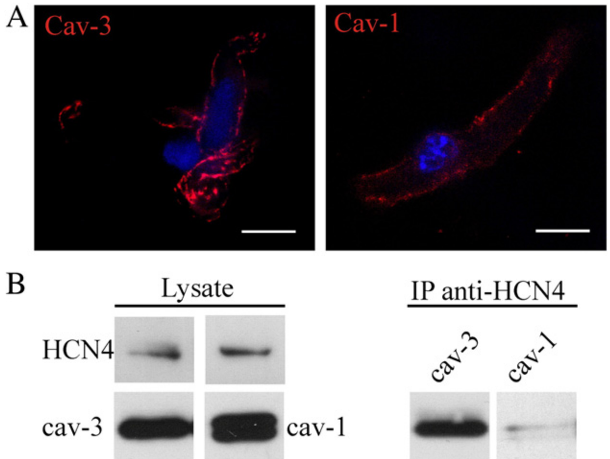

Fig. 1. Expression of caveolin-1 and -3 in mouse SAN cells. A, Single confocal images of SAN myocytes, showing the expression of cav-3 and cav-1 (red, as indicated). Nuclei were stained by DAPI; calibration bars 10 μm. B left, Western blot of the SAN lysates showing the bands for HCN4, cav-3 and cav-1 at the expected molecular weight; right, Western blot of proteins immunoprecipitated using an anti-HCN4 antibody (IP-HCN4) and immunoblotted with the anti-cav-3 and anti-cav-1 antibodies. (For interpretation of the references to color in this figure legend, the reader is referred to the web version of this article.)

Current traces recorded during application of a hyperpolarizing 2-step protocol (−85/−135; holding potential −20 mV) in cells expressing the rbHCN4 WT, Y259S and Y259F channels are shown in Fig. 2B. Compared to WT, the Y259S current had much faster activation and slower deactivation kinetics; also, the Y259S current was fully activated at −85 mV, as apparent from the lack of extra current activation when stepping from −85 to −135 mV, indicating a displacement of the activation range to more depolarized voltages. The introduction of a different aromatic residue in position 259 (Y259F), on the other hand, resulted in currents with kinetics similar to those of WT channels.

The above observations were confirmed and quantified by analyzing the mean activation curves and activation/deactivation τ of WT, Y259S and Y259F mutant channels. Plots of the mean activation curves (Fig. 2C left) show that Y259S channels (open circles) activate at significantly more positive potentials than WT channels (filled circles), while the activation curve of Y259F mutants (open squares) does not differ significantly from that of WT channels (for values see Supplementary Table 1).

Both the activation and deactivation τ curves of Y259S mutants were also shifted to more positive potentials compared to WT channels (Fig. 2C right), resulting in faster activation and slower deactivation kinetics (Supplementary Table 1) over the whole range of potentials tested ($p<0.05$). The voltage dependence of τ curves of Y259F mutant channels was essentially identical to that of WT channels.

Similar results were obtained from the analysis of the mutations at position 262. As shown in Fig. 2D, current traces recorded from CHO cells transfected with WT, F262V and F262Y channels indicate that removal of this aromatic residue caused a depolarizing shift of the activation curve. In Fig. 2E left, measurement of mean activation curves shows that the F262V mutant channels (open triangles) indeed activated at more positive potentials than WT (dashed line) and F262Y channels (inverted open triangles). Interestingly, the activation τ curve of F262V was essentially coincident with that of WT channels, while the deactivation τ curve was shifted to more positive potentials by about 20 mV ($p<0.05$, Fig. 2E right and Supplementary Table 1). The τ curves of F262Y mutant channels, on the other hand, did not deviate significantly from those of WT channels.

3.3. Caveolar disorganization has no effect on channels with a disrupted CBD

Previous work in both native SAN myocytes and HCN4-transfected HEK293 cells has shown that lipid rafts disorganization by cholesterol depletion causes a positive shift of the activation curve and a slowing of deactivation [16]. Since the effects of the mutations of the CBD investigated above are qualitatively similar to those previously reported upon disorganization of lipid raft/caveolae, we evaluated the effects of cholesterol depletion, caused by 1% MβCD, on WT and mutant currents (Fig. 3). Incubation of cells expressing WT HCN4 channels with MβCD shifted the activation curve to more positive potentials compared to untreated cells (Fig. 3, Supplementary Table 2). Furthermore, in agreement with previously reported data, cholesterol depletion significantly slowed deactivation τ in the range of potentials between −75 and −25 mV (Supplementary Table 2). When cells transfected with either the Y259S or the F262V mutant channels were treated with MβCD, no changes were observed in either activation curves or deactivation τ (Fig. 3, Supplementary Table 2).

The cholesterol-depletion procedure was effective, on the other hand, when applied to cells transfected with either the Y259F or F262Y mutants (Fig. 3, Supplementary Table 2).

These results demonstrate that disruption of the CBD is sufficient to abolish the functional effect of caveolae disorganization mediated by cholesterol depletion, supporting the idea that the interaction of HCN4 channels with caveolar proteins is mediated by the CBD; indeed kinetic properties of channels with a preserved CBD become more similar to those of Y259S and F262V mutants after caveolar disorganization.

Since the CBD is conserved in all HCN isoforms, we tested whether caveolar disorganization could alter also the kinetics of HCN1 channels. As shown in the two bottom panels of Fig. 3, MβCD treatment caused a substantial shift of the activation curve to more positive voltages and slowed the deactivation time constants of CHO cells transfected with the mouse (m)HCN1 channels (for values see Supplementary Table 2).

3.4. HCN4 mutants present normal cAMP sensitivity

We showed previously that although cholesterol depletion causes a positive shift of HCN4 activation curve, it does not impair the physiological modulation of the channel by cyclic nucleotides [16]. To analyze if mutant channels retain a normal cAMP sensitivity, activation curves were measured under control conditions and in the presence of a saturating concentration of cAMP (10 μM) in the recording pipette. All types of channels were found to be normally sensitive to cAMP (Supplementary Table 3).

3.5. CBD disruption affects HCN4 channel trafficking to the plasma membrane

As well as modifying current kinetics, mutations of the CBD caused a significant decrease in current density. In Fig. 4A representative current traces, normalized to cell capacitance, are shown for wild-type and mutant channels, as indicated. Bar graph plots of mean current densities in Fig. 4B show that the Y259S and F262V mutants generated current densities significantly smaller than the WT channels ($p<0.05$), while Y259F and F262Y mutant channels were expressed as efficiently as WT channels.

To check if the decrease in current density derived from a decrease in the number of functional channels expressed on the plasma membrane, we ran immunofluorescence experiments on CHO cells transfected with the various constructs so as to visualize potential channel mislocalization. As apparent in Fig. 4C from the representative single confocal images of HCN4-labeled cells (left) and the corresponding surface plot (middle), mutant constructs characterized by poor current density (Y259S and

Please cite this article as: Barbuti A, et al, Original articleA caveolin-binding domain in the HCN4 channels mediates functional interaction with caveolin proteins, J Mol Cell Cardiol (2012), doi:10.1016/j.yjmcc.2012.05.013

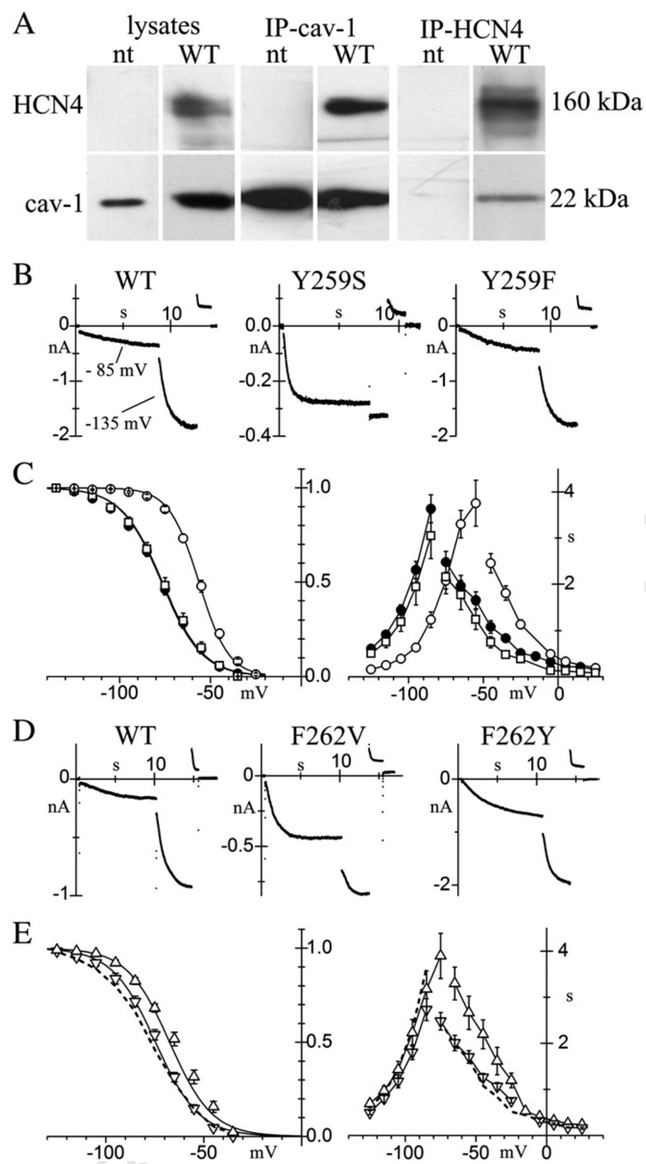

Fig. 2. Comparison of kinetic properties of WT and mutated HCN4 channels. A, Western blot of the lysates and of the proteins immunoprecipitated using anti-HCN4 (IP-HCN4) or anti-cav-1 (IP-cav-1) antibodies, obtained from non-transfected (nt) CHO cells or from cells transfected with the wild-type HCN4 construct (WT). B, representative current traces recorded from CHO cells transfected with WT, Y259S and Y259F HCN4 channels, during a two-step protocol to the voltages indicated. C, Mean activation curves (left) and τ curves of WT (filled circles, n = 37), Y259S (open circles, n = 35) and Y259F (open squares, n = 21) HCN4 channels. D, representative current traces recorded from cells expressing WT, F262V and F262Y channels. E, Mean activation (left) and τ curves (right) of F262V (triangles) and F262Y (inverted triangles); WT curves (dashed lines) are the same as in B.

F262V) also displayed reduced membrane expression and intracellular accumulation of HCN4 channels.

Expression density profiles in the right panels, corresponding to the dotted line scans in left panels, show that the intracellular HCN4 (green) and the nuclear signals (blue) do not overlap, indicating that HCN4 is accumulated in the cytoplasm. An analysis of the fluorescence density in the membrane and in the cytosol was carried out to quantify the different distribution of HCN4 between these two compartments. Mean values of ratios between membrane and cytosol fluorescence intensity are plotted in Fig. 4D; in comparison to WT cells (1.82 ± 0.21 n = 29), cells expressing Y259S and F262V mutants show significantly reduced ratios (0.8 ± 0.11 n = 19 and 0.99 ± 0.17, n = 20, respectively, $p<0.05$) while ratios in cells expressing Y259F and F262Y channels (1.7 ± 0.48, n = 8 and 2.09 ± 0.56, n = 13, respectively) are similar to that in WT cells. These data indicate that the lower current density of Y259S and F262V mutants is due to a reduced membrane localization of channels likely due to a defective trafficking to the plasma membrane caused by lack of interaction with caveolin. In fact, in CHO cells expressing the WT HCN4 channels, acute caveolar disorganization by MβCD neither altered membrane distribution (Supplementary Fig. 3) nor decreased current density (MbCD-treated cells: −79.8 ± 16.9 pA/pF, n = 12; untreated day-matched cells: −78.3 ± 21.8 pA/pF, n = 8), confirming previous observations in HEK cells and native SAN myocytes [16].

3.6. HCN4 mutants with a disrupted CBD accumulate in the Golgi complex

Since it is known that caveolar/lipid raft protein complexes assemble in the Golgi apparatus [20,21] and lack of caveolin cause intracellular/Golgi accumulation of such proteins [22], we next investigated the subcellular localization of cytoplasmic channels. Representative confocal images of CHO cells double labeled with anti-GM130, a marker of the Golgi apparatus (red), and anti HCN4 antibodies (green) are shown in Fig. 5. Co-localization of the two signals (yellow) indicates that Y259S

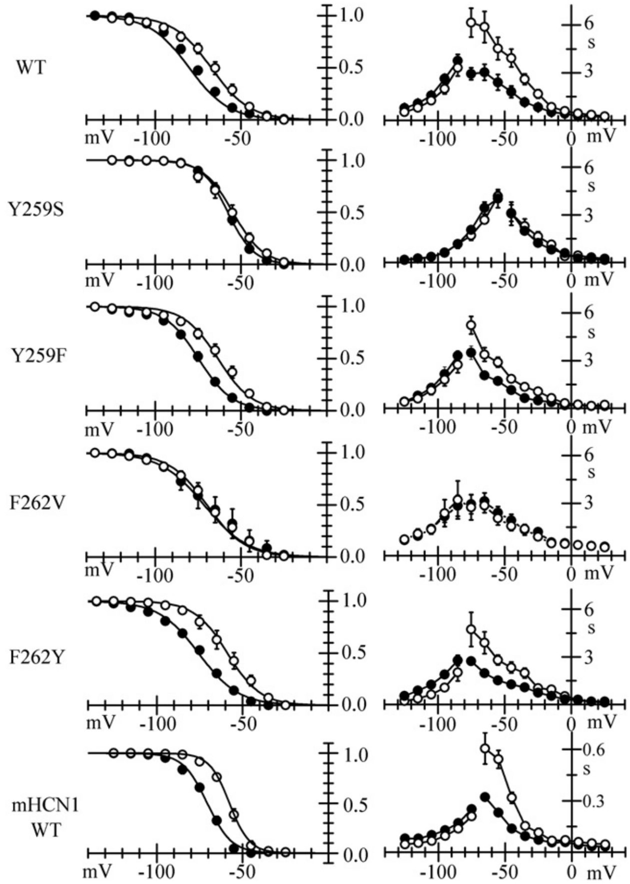

Fig. 3. Effects of caveolae disorganization. Activation (left) and τ curves (right) of the WT and mutant HCN4 and WT HCN1 channels recorded in MβCD-treated (open circles) and day-matched untreated cells (filled circles). For values see Section 3.3 and Supplementary Table 2.

and F262V but not WT, Y259F and F262Y channels, are indeed retained in the Golgi apparatus.

3.7. Alteration of the CBD impairs HCN4–cav-1 interaction

We also assessed if the interaction between HCN4 and cav-1 is affected by mutation of the CBD. Lysates obtained from CHO cells transfected with either WT or mutated HCN4 channels (Fig. 6A) were immunoprecipitated with an anti-cav-1 antibody and the presence of HCN4 in the precipitated proteins was evaluated (Fig. 6B).

The amount of precipitated HCN4, calculated by densitometry analysis, was normalized to the amount of HCN4 in the corresponding lysate to account for variability in transfection efficiency. The mean bar graph in Fig. 6C shows that significantly less HCN4 was precipitated when the CBD was altered, in accordance with a weaker interaction with cav-1. A similar pattern was evident when evaluating cav-1 expression in the proteins immunoprecipitated with anti-HCN4 antibody (Fig. 6D).

3.8. HCN4 functional alterations in caveolin-free fibroblasts

We then carried out experiments using mouse embryonic fibroblasts derived from cav-1 knockout animals (caveolin-free mef) which lack any caveolin (Supplementary Fig.2). When WT and mutated HCN4 channels were expressed in caveolin-free mef, only a fraction of cells displayed a measurable HCN4 current (34.6%, 3.9%, 46.1%, 21.9% and 12.7% for WT, Y259S, Y259F, F262V and F262Y-expressing cells, respectively). Analysis of the current densities in the fraction of HCN4-expressing caveolin-free mef yielded values significantly lower than those recorded in CHO cells expressing WT, Y259F and F262Y channels (-17.6 ± 4.2 n = 18; -17.9 ± 4.2 n = 14; -6.5 ± 2.3 n = 8; $p<0.05$) but not Y259S and F262V channels (-6.0 ± 4.1 n = 3, -14.3 ± 3.0, n = 9 respectively; $p>0.05$). Furthermore, current densities of the various mutants were not different from WT, in caveolin-free mef. Immunofluorescence analysis of caveolin-free mef revealed that all HCN4 constructs were abundantly expressed, but remained mostly confined to the cytoplasm (Fig. 7).

Analysis of current kinetics revealed that the activation curve of F262V channels was similar to those of WT and F262Y, while that of Y259S was depolarized by about 11 mV relative to those of WT channels (Fig. 7, bottom right); the 11 mV shift was smaller than that observed in CHO cells (20.1 mV). These data agree with a role of caveolins in modulating the voltage dependence of HCN4 channels, and suggest that the Y259S mutation may also affect the HCN4 channel properties in a caveolin-independent manner.

4. Discussion

All four HCN isoforms (HCN1-4) are found in cardiac tissues, though with different, region-specific degrees of expression; however, heteromeric assembly of different subunits to form functional tetrameric channels fails to fully reproduce the cardiac I_f current.

Data from various species indicate that HCN4 is the most highly expressed isoform in the SAN [5–7]. However, heterologously expressed HCN4 channels generate currents activating at more negative potentials and with slower kinetics than the native SAN I_f; also, expression of heteromeric HCN4/HCN1 or HCN4/HCN2 constructs again failed to fully recapitulate I_f [9,23]. These data naturally lead to the consideration that the properties of native channels may be profoundly modulated by the intracellular environment [24,25] and indeed there is growing evidence that the interaction with partner proteins is important in setting the functional properties of native currents [10–15].

We have previously shown that the interaction of SAN f-channels with cav-3 strongly affects basal channel functions and its modulation [12,16] and that such interaction is also apparent when HCN4 channels are heterologously expressed with cav-3 in HEK cells [13]. However, the molecular mechanism responsible for the interaction between HCN4 channels and caveolins has not been identified.

A potential CBD (**W**IIHP**Y**SD**F**), highly conserved through evolution from urochordates to vertebrates, is present at the N-terminus of all HCN isoforms (Supplementary Fig. 1). Interestingly, the corresponding interacting sequence (caveolin-scaffolding domain) of cav-1 and cav-3 is also similarly conserved (see [18] and Supplementary Fig. 4). Although the presence of a CBD does not automatically imply an interaction with caveolins, a direct involvement of this motif has been demonstrated for several proteins, including G proteins (Gi2α), Src kinases, EGF-receptors, eNOS, PKCα, K_{ATP} channels and MaxiK channels [18,19,27–29].

Although in SAN cells cav-3 seems to be the predominant isoform, we have shown here that SAN myocytes express also the ubiquitous cav-1 isoform and that HCN4 channels can interact with both these subunits; evidence for the expression of cav-1 in cardiomyocytes is in agreement with recent data showing that both atrial and ventricular cardiomyocytes express both caveolins [30,31]. Because both cav-1 and cav-3 are expressed in SAN and because exogenous expression of either cav-1 or cav-3 in caveolin-null cells rescues the trafficking defects of GPI-anchored proteins caused by the lack of caveolae [22], we have chosen to investigate the role of the CBD of HCN4 channels in CHO cells which express cav-1.

Here we have shown that disruption of the CBD of HCN4 causes changes in the channel kinetics which are similar to those previously reported for caveolae disorganization by cholesterol depletion [12,16]. Relative to WT channels, Y259S and F262V mutant channels, in which an aromatic residue is substituted, are characterized by positively

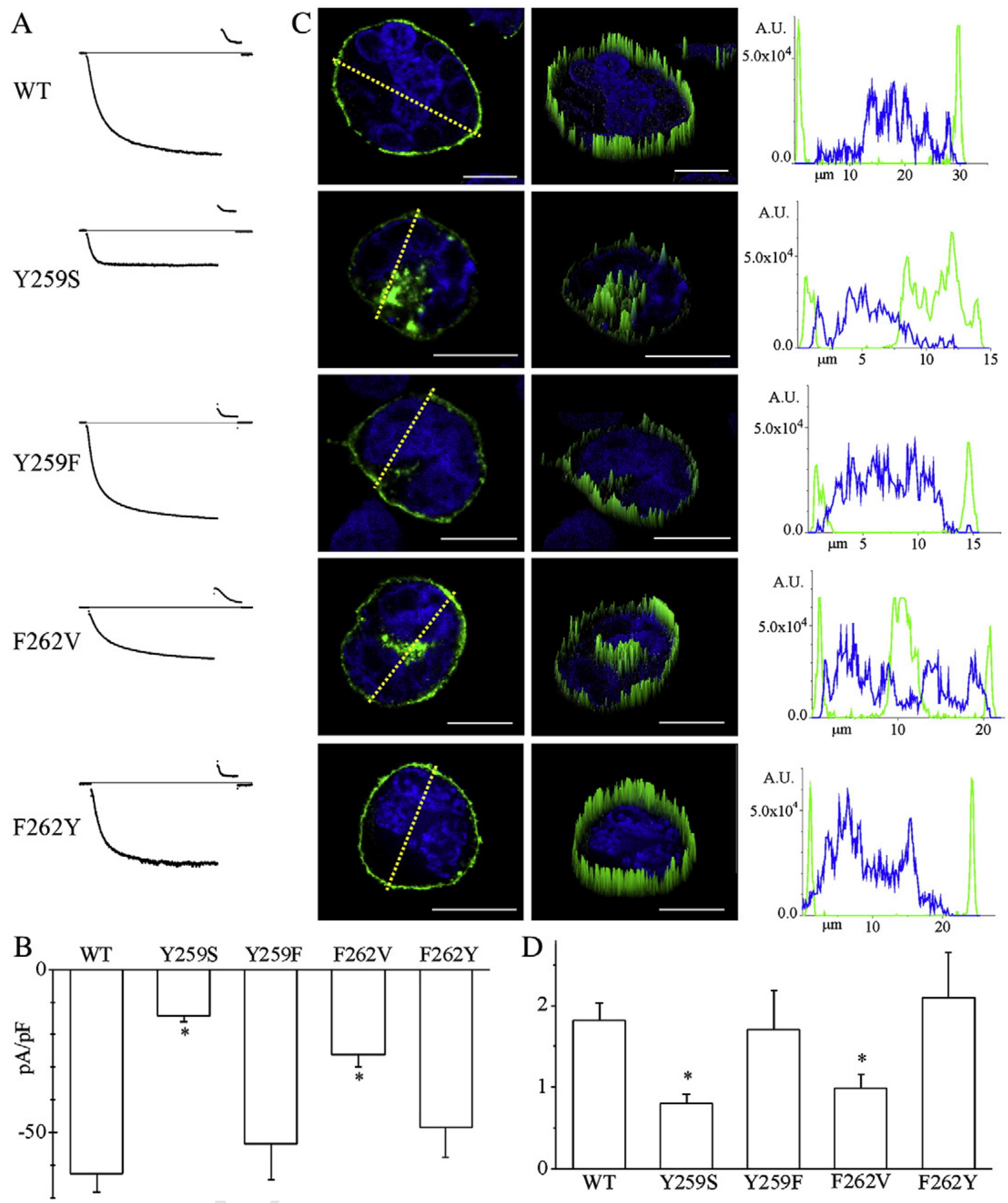

Fig. 4. Expression levels of WT and HCN4 mutant channels. A, representative current traces recorded during steps from −20 to −125 mV in cells expressing WT and mutant HCN4 channels. B, Mean current densities for the various HCN4 constructs; values were: −63.7 ± 5.5 (n = 44), −14.1 ± 1.8 (n = 49), −26.1 ± 3.8 (n = 28), −56.6 ± 11.4 pA/pF (n = 32) and −48.2 ± 7.1 (n = 24) for WT, Y259S, F262V, Y259F and F262Y channels, respectively. C, Single confocal images (left) showing the distribution of HCN4 staining (green) in CHO cells transfected with WT or mutant channels. Dashed lines represent cell planes used to generate the expression density profiles in the right panels. Mid panels represent surface plots (by Image-Pro® Plus 6.0) in which the signal height is proportional to the signal intensity of left panels. Nuclei were stained by DAPI. Calibration bar, 10 μm. D, Mean values of the membrane-to-cytosol fluorescence intensity ratios; asterisks in B and D indicate $p < 0.05$. (For interpretation of the references to color in this figure legend, the reader is referred to the web version of this article.)

shifted activation curves and slower deactivation time constants. In contrast, channels with mutations that preserve the aromatic residues in the proper positions (Y259F and F262Y) have kinetics similar to those of WT channels. This observation rules against a conformational, unspecific effect of the amino acid substitution on channel function. The specific involvement of this consensus motif in HCN4-caveolin interaction is further supported by the fact that MβCD-mediated cholesterol depletion, a treatment known to disorganize membrane caveolae, is effective on WT, Y259F and F262Y HCN4 channels and also on HCN1 channels, but has no effect on HCN4 channels with a disrupted motif (Y259S and F262V).

Previous work from our laboratory has shown that the intracellular application of the unspecific protease pronase causes a large and irreversible positive shift (56 mV) of f-channel activation and makes the channel insensitive to cAMP, highlighting the existence of a basal inhibitory action of intracellular portions of the channel on its opening that is removed by cAMP [32]; a later study [33] showed that complete deletion of the C-terminus of HCN2 channels completely abolishes cAMP sensitivity but causes a more reduced positive shift of the activation curve (24 mV), suggesting that some other mechanism must be involved to explain the remaining ~30 mV shift caused by pronase. Here we show that a single amino acid substitution in the

Please cite this article as: Barbuti A, et al, Original articleA caveolin-binding domain in the HCN4 channels mediates functional interaction with caveolin proteins, J Mol Cell Cardiol (2012), doi:10.1016/j.yjmcc.2012.05.013

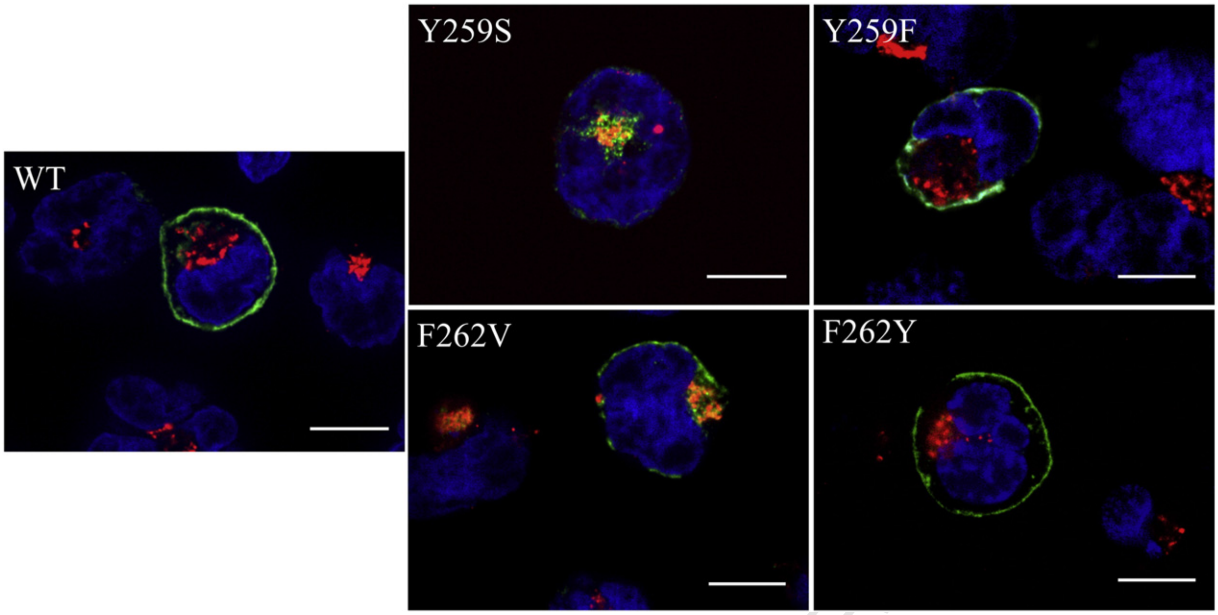

Fig. 5. Intracellular HCN4 is retained in the Golgi apparatus. Single confocal images of CHO cells transfected with WT or mutant channels. Intracellular HCN4 (green) and GM-130 (red), co-localize (yellow) in cells expressing the Y259S, and F262V channels, but not in cells expressing WT, Y259F and F262Y channels. Nuclei stained by DAPI; calibration bars 10 μm. (For interpretation of the references to color in this figure legend, the reader is referred to the web version of this article.)

N-terminus of HCN4 can produce a substantial depolarizing shift of HCN4 activation while retaining normal cAMP sensitivity. We can thus speculate that part of the large shift caused by internal pronase perfusion can be ascribed to the disruption of the HCN channel–caveolin interaction caused by the proteolytic cleavage of the CBD.

Although acute disruption of caveolae does not affect the I_f current amplitude [16], we found that mutation of the CBD also affects the expression of HCN4 channels. It is known that full deletion of the N-terminus, or deletion of a conserved 52 amino acid-long region adjacent to the first transmembrane (S1) domain of the mouse HCN2, results in lack of current expression and in perinuclear accumulation of HCN proteins [34,35], indicating that the N-terminus is important for proper membrane trafficking/expression. Based on the evidence that CHO cells expressing Y259S or F262V channels display an expression pattern similar to that of N-terminus-deleted channels and that HCN4 channels expression is severely depressed in caveolin-free mef, we can speculate that interactions between the CBD and caveolin mediate channel trafficking to or retention into the plasma membrane. The accumulation of the HCN4 channels with an altered CBD in the Golgi apparatus of CHO cells and the evidence that acute caveolar disruption neither alters current density nor membrane localization of HCN4 (Supplementary Fig.3), are in agreement with the notion that caveolar protein complexes form in that compartment and from there are transported to the plasma membrane [20,21]. Moreover, the CBD-independent intracellular distribution of HCN4, is consistent with previous evidence that glycosylphosphatidyl inositol-linked proteins, which are normally localized into caveolae, are retained in the Golgi complex when expressed in cav-1 null cells [22].

Some of the proteins that interact with caveolin similarly show a decreased expression when their interacting sequences are modified [28,29,36]. Slo1, for example, the α-subunit of the Maxi K potassium channel, is not transferred to the plasma membrane when its CBD is deleted, as shown by the complete absence of membrane labeling and recorded current [28].

Beside affecting the expression levels of HCN4 channels, the HCN4–caveolin interaction has a role in setting the position of channel activation, as indicated by evidence that impairment of this interaction, either chemical (due to MβCD-mediated caveolae disorganization) or structural

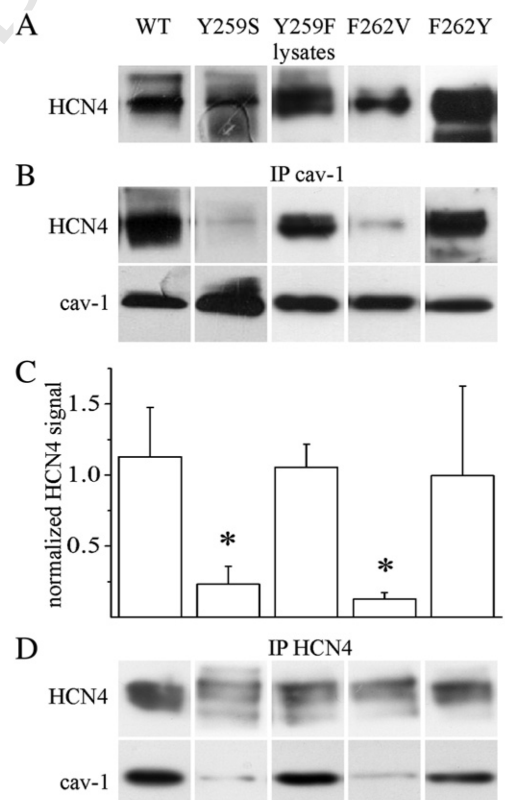

Fig. 6. Alteration of the CBD weakens HCN4–caveolin-1 interactions. A, blots showing the presence of HCN4 in lysates obtained from CHO cells transfected with either WT or mutated channels. B, representative blots showing a reduced amount of HCN4 immunoprecipitated by cav1 in cells expressing Y259S and F262V mutants. HCN4 expression levels in the IP cav1 (B) were normalized to HCN4 signals detected in the corresponding cell lysates (A) to account for differences in the transfection efficiency. C, mean bar graph showing the amount of normalized HCN4 precipitated by cav-1 ($n \geq 3$, * $p < 0.05$). D, representative blots showing that when proteins are immunoprecipitated by HCN4, a reduced cav-1 expression level is detected in the Y259S and F262V lanes.

Please cite this article as: Barbuti A, et al, Original articleA caveolin-binding domain in the HCN4 channels mediates functional interaction with caveolin proteins, J Mol Cell Cardiol (2012), doi:10.1016/j.yjmcc.2012.05.013

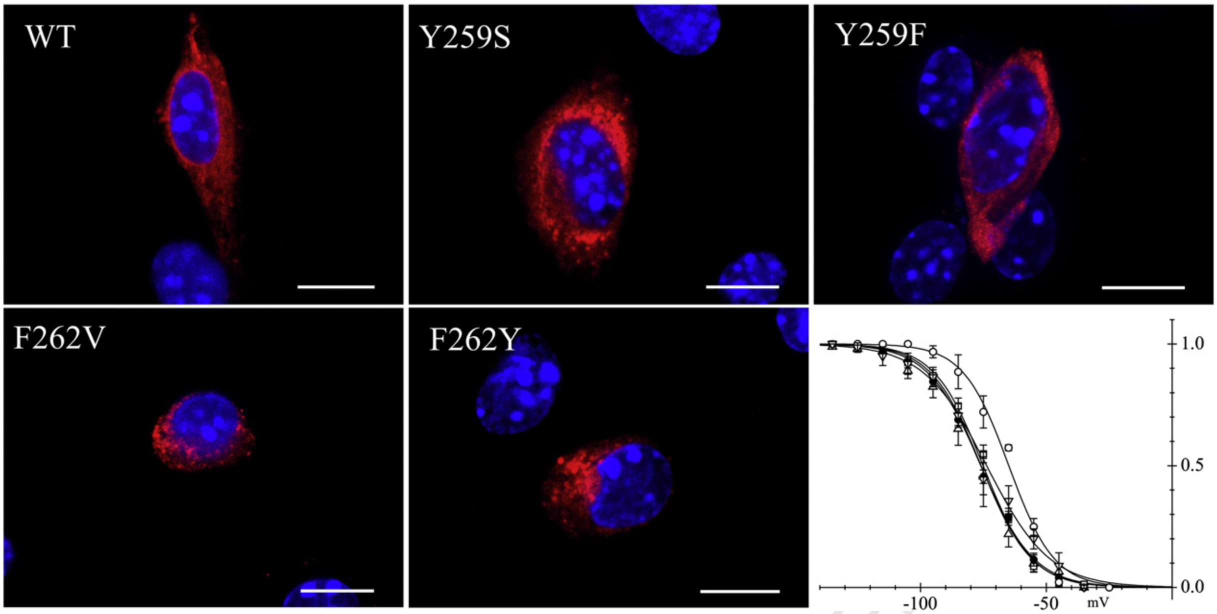

Fig. 7. Expression and functional properties of HCN4 channels in caveolin-free mef. Single confocal images of caveolin-free mef transfected with WT or mutant channels, labeled with an anti-HCN4 (red) antibody. Nuclei stained by DAPI; calibration bars 10 μm. The lower right panel shows the mean activation curves of WT (filled circles), Y259F (open squares), F262V (triangles) and F262Y (inverted triangles) channels. Half-activation voltages (V_{half}) and inverse-slope factors (s) from Boltzmann curve fitting were −76.0 ± 1.3 and 10.5 ± 0.6 mV (WT, n = 17), −64.9 ± 1.4 and 9.0 ± 1.4 (Y259S, n = 3, $p < 0.05$), −75.1 ± 1.2 and 9.7 ± 0.8 mV (Y259F, n = 11), −75.9 ± 2.6 and 10.0 ± 1.0 mV (F262V, n = 6), −73.7 ± 2.4 and 12.5 ± 1.0 mV (F262Y, n = 5).

(due to mutation of the interacting sequence) shifts the channel activation curve by about 10 mV. This depolarizing shift is lost when MβCD is applied to cells expressing the Y259S and F262V channels or when these channels are expressed in caveolin-free mef. The presence of a more depolarized activation for the Y259S mutant in caveolin-free mef suggests that part of the positive shift found when this mutant is expressed in CHO cells may reflect a molecular mechanism unrelated to HCN–caveolin interaction. Interestingly, Liu and Aldrich have recently identified a conserved arginine and lysine-rich functional domain within the N-Terminus of the HCN4 whose mutation causes significant alterations of the channel kinetic properties and suggested that these effects are due to a modification in the electrostatic interactions either with other portions of the channels or with other partner proteins [37].

It has been shown that inherited cav-3 mutations may lead to functional changes in ion channels located in caveolae which cause long QT syndrome and sudden infant death syndrome (SIDS) [38]; cav-3 mutations can also cause hypertrophic cardiomyopathy and these conditions can in turn cause ion channels dysfunction [38]. A more detailed understanding of the molecular mechanisms underlying HCN–caveolin interaction and the consequences caused by the disruption of such interaction may help to provide a deeper insight into the arrhythmogenic risk of specific cardiac disorders. It may be noted that while the loss of interaction between HCN4 and caveolin decreases the fraction of channels available on the membrane, it also increases the current available at a given potential due to the positive shift of the activation curve. The overall effect on cellular excitability will thus depend on the balance between these two contrasting actions.

5. Conclusions

In conclusion we have shown the presence of a highly conserved Caveolin-Binding Domain at the N-terminus of HCN4 channels; mutations altering the aromatic residue composition of this CBD cause kinetic changes similar to those caused by the caveolar disorganization mediated by cholesterol depletion, a treatment that becomes ineffective in such mutants; mutations of the CBD also impair channel trafficking to the plasma membrane. These data support a fundamental role of the cellular microenvironment for proper function of the pacemaker HCN4 channel.

Supplementary data to this article can be found online at http://dx.doi.org/10.1016/j.yjmcc.2012.05.013.

Acknowledgments Q3

This work was supported by: Fondo per gli Investimenti della Ricerca di Base [FIRB RBLA035A4X], European Union [Normacor CT2006-018676] and Ministero Affari Esteri [MAE Prot.269/P/0120422] to DD.

Disclosures

None declared.

Uncited reference Q5

[26]

References

[1] DiFrancesco D. Pacemaker mechanisms in cardiac tissue. Annu Rev Physiol 1993;55:455–72.
[2] Barbuti A, DiFrancesco D. Control of cardiac rate by “funny” channels in health and disease. Ann N Y Acad Sci 2008;1123:213–23.
[3] DiFrancesco D. The role of the funny current in pacemaker activity. Circ Res 2010;106:434–46.
[4] Barbuti A, Baruscotti M, DiFrancesco D. The pacemaker current: from basics to the clinics. J Cardiovasc Electrophysiol 2007;18:342–7.
[5] Liu J, Dobrzynski H, Yanni J, Boyett MR, Lei M. Organisation of the mouse sinoatrial node: structure and expression of HCN channels. Cardiovasc Res 2007;73:729–38.
[6] Yamamoto M, Dobrzynski H, Tellez J, Niwa R, Billeter R, Honjo H, et al. Extended atrial conduction system characterised by the expression of the HCN4 channel and connexin45. Cardiovasc Res 2006;72:271–81.
[7] Chandler NJ, Greener ID, Tellez JO, Inada S, Musa H, Molenaar P, et al. Molecular architecture of the human sinus node: insights into the function of the cardiac pacemaker. Circulation 2009;119:1562–75.
[8] Brioschi C, Micheloni S, Tellez JO, Pisoni G, Longhi R, Moroni P, et al. Distribution of the pacemaker HCN4 channel mRNA and protein in the rabbit sinoatrial node. J Mol Cell Cardiol 2009;47:221–7.
[9] Altomare C, Terragni B, Brioschi C, Milanesi R, Pagliuca C, Viscomi C, et al. Heteromeric HCN1-HCN4 channels: a comparison with native pacemaker channels from the rabbit sinoatrial node. J Physiol (Lond) 2003;549:347–59.
[10] Yu H, Wu J, Potapova I, Wymore RT, Holmes B, Zuckerman J, et al. MinK-related peptide 1: a beta subunit for the HCN ion channel subunit family enhances expression and speeds activation. Circ Res 2001;88:E84–7.

[11] Decher N, Bundis F, Vajna R, Steinmeyer K. KCNE2 modulates current amplitudes and activation kinetics of HCN4: influence of KCNE family members on HCN4 currents. Pflugers Arch 2003;446:633–40.
[12] Barbuti A, Terragni B, Brioschi C, DiFrancesco D. Localization of f-channels to caveolae mediates specific beta2-adrenergic receptor modulation of rate in sinoatrial myocytes. J Mol Cell Cardiol 2007;42:71–8.
[13] Ye B, Balijepalli RC, Foell JD, Kroboth S, Ye Q, Luo YH, et al. Caveolin-3 associates with and affects the function of hyperpolarization-activated cyclic nucleotide-gated channel 4. Biochemistry 2008;47:12312–8.
[14] Michels G, Er F, Khan IF, Endres-Becker J, Brandt MC, Gassanov N, et al. K+ channel regulator KCR1 suppresses heart rhythm by modulating the pacemaker current If. PLoS One 2008;3:e1511.
[15] Peters CJ, Chow SS, Angoli D, Nazzari H, Cayabyab FS, Morshedian A, et al. In situ co-distribution and functional interactions of SAP97 with sinoatrial isoforms of HCN channels. J Mol Cell Cardiol 2009;46:636–43.
[16] Barbuti A, Gravante B, Riolfo M, Milanesi R, Terragni B, DiFrancesco D. Localization of pacemaker channels in lipid rafts regulates channel kinetics. Circ Res 2004;94:1325–31.
[17] Steinberg SF, Brunton LL. Compartmentation of G protein-coupled signaling pathways in cardiac myocytes. Annu Rev Pharmacol Toxicol 2001;41:751–73.
[18] Couet J, Li S, Okamoto T, Ikezu T, Lisanti MP. Identification of peptide and protein ligands for the caveolin-scaffolding domain. Implications for the interaction of caveolin with caveolae-associated proteins. J Biol Chem 1997;272:6525–33.
[19] Razani B, Woodman SE, Lisanti MP. Caveolae: from cell biology to animal physiology. Pharmacol Rev 2002;54:431–67.
[20] Harder T, Simons K. Caveolae, DIGs, and the dynamics of sphingolipid-cholesterol microdomains. Curr Opin Cell Biol 1997;9:534–42.
[21] Tagawa A, Mezzacasa A, Hayer A, Longatti A, Pelkmans L, Helenius A. Assembly and trafficking of caveolar domains in the cell: caveolae as stable, cargo-triggered, vesicular transporters. J Cell Biol 2005;170:769–79.
[22] Sotgia F, Razani B, Bonuccelli G, Schubert W, Battista M, Lee H, et al. Intracellular retention of glycosylphosphatidyl inositol-linked proteins in caveolin-deficient cells. Mol Cell Biol 2002;22:3905–26.
[23] Whitaker GM, Angoli D, Nazzari H, Shigemoto R, Accili EA. HCN2 and HCN4 isoforms self-assemble and co-assemble with equal preference to form functional pacemaker channels. J Biol Chem 2007;282:22900–9.
[24] Qu J, Barbuti A, Protas L, Santoro B, Cohen IS, Robinson RB. HCN2 overexpression in newborn and adult ventricular myocytes: distinct effects on gating and excitability. Circ Res 2001;89:E8–14.
[25] Qu J, Altomare C, Bucchi A, DiFrancesco D, Robinson RB. Functional comparison of HCN isoforms expressed in ventricular and HEK 293 cells. Pflugers Arch 2002;444:597–601.
[26] Qu J, Kryukova Y, Potapova IA, Doronin SV, Larsen M, Krishnamurthy G, et al. MiRP1 modulates HCN2 channel expression and gating in cardiac myocytes. J Biol Chem 2004;279:43497–502.
[27] Couet J, Sargiacomo M, Lisanti MP. Interaction of a receptor tyrosine kinase, EGF-R, with caveolins. Caveolin binding negatively regulates tyrosine and serine/threonine kinase activities. J Biol Chem 1997;272:30429–38.
[28] Alioua A, Lu R, Kumar Y, Eghbali M, Kundu P, Toro L, et al. SLO1 caveolin-binding motif, a mechanism of caveolin-1–SLO1 interaction regulating SLO1 surface expression. J Biol Chem 2007;283:4808–17.
[29] Brainard AM, Korovkina VP, England SK. Disruption of the maxi-K–caveolin-1 interaction alters current expression in human myometrial cells. Reprod Biol Endocrinol 2009;7:131.
[30] Volonte D, McTiernan CF, Drab M, Kasper M, Galbiati F. Caveolin-1 and caveolin-3 form heterooligomeric complexes in atrial cardiac myocytes that are required for doxorubicin-induced apoptosis. Am J Physiol Heart Circ Physiol 2008;294:H392–401.
[31] Cho WJ, Chow AK, Schulz R, Daniel EE. Caveolin-1 exists and may function in cardiomyocytes. Can J Physiol Pharmacol 2010;88:73–6.
[32] Barbuti A, Baruscotti M, Altomare C, Moroni A, DiFrancesco D. Action of internal pronase on the f-channel kinetics in the rabbit SA node. J Physiol 1999;520(Pt 3):737–44.
[33] Wainger BJ, DeGennaro M, Santoro B, Siegelbaum SA, Tibbs GR. Molecular mechanism of cAMP modulation of HCN pacemaker channels. Nature 2001;411:805–10.
[34] Proenza C, Tran N, Angoli D, Zahynacz K, Balcar P, Accili EA. Different roles for the cyclic nucleotide binding domain and amino terminus in assembly and expression of hyperpolarization-activated, cyclic nucleotide-gated channels. J Biol Chem 2002;277:29634–42.
[35] Tran N, Proenza C, Macri V, Petigara F, Sloan E, Samler S, et al. A conserved domain in the NH2 terminus important for assembly and functional expression of pacemaker channels. J Biol Chem 2002;277:43588–92.
[36] Kong MM, Hasbi A, Mattocks M, Fan T, O'Dowd BF, George SR. Regulation of D1 dopamine receptor trafficking and signaling by caveolin-1. Mol Pharmacol 2007;72:1157–70.
[37] Liu H, Aldrich RW. Tissue-specific N terminus of the HCN4 channel affects channel activation. J Biol Chem 2011;286:14209–14.
[38] Gazzerro E, Sotgia F, Bruno C, Lisanti MP, Minetti C. Caveolinopathies: from the biology of caveolin-3 to human diseases. Eur J Hum Genet 2010;18:137–45.

Please cite this article as: Barbuti A, et al, Original articleA caveolin-binding domain in the HCN4 channels mediates functional interaction with caveolin proteins, J Mol Cell Cardiol (2012), doi:10.1016/j.yjmcc.2012.05.013